# Lipid Tempering Simulation of Model Biological Membranes on Parallel Platforms

Chiara Cardelli

*Computational Physics Dept., University of Wien, Sensengasse 8/9 1090 Wien, Austria*

Alessandro Barducci

*Centre de Biochimie Structurale de Montpellier, 29 rue de Navacelles 34090, Montpellier, France*

Piero Procacci

*Chemistry Dept., University of Florence, Via Lastruccia 3 50019 Sesto Fiorentino, Italy*

**Abstract**

In this report we have tested a parallel implementation for the simulation of lipid bilayers at the atomistic level, based on a generalized ensemble protocol where only the torsional degrees of freedom of the alkyl chains of the lipids are heated. The results in terms of configurational sampling enhancement have been compared with a conventional simulation produced with a widespread molecular dynamics code. Results show that the proposed thermodynamic-based multiple trajectories parallel protocol for membrane simulations allows for an efficient use of CPU resources with respect to the conventional single trajectory, providing accurate results for area and volume per lipid, membrane thickness, undulation spectra and boosting significantly diffusion and mixing in lipid bilayers due to the sampling enhancement of *gauche/trans* ratios of the alkyl chain dihedral angles.

*Keywords:* POPC, Molecular Dynamics, Hamiltonian Replica Exchange Simulation (HREM), gauche/trans ratio, Slipids

*Email address:* procacci@unifi.it (Piero Procacci)

## 1. Introduction

Molecular dynamics simulation is an important computational tool for the study of biomolecular systems, such as biological membranes, that have lipid bilayers as main constituents.[1] The recent development of high performance massively parallel computing environments (HPC) exploiting high speed communication links has nowadays made possible parallel simulations in the time range of hundreds of nanosecond of lipid bilayers of the extension of tens nanometers. In spite of the indisputable and tremendous gain in the performance with respect to early serial applications, computational scientists still face a severe length-scale and a time-scale problem in membrane simulation. The current limits in length and time scale in fully atomistic simulations (20-30 nm and $\simeq 1$ $\mu$s respectively) severely restrain the possibility of studying key properties of bilayers like the bending rigidity via determination of the undulation spectrum and/or cooperative transport phenomena. Both these properties are intimately connected with important biological situations including endocytosis, lipid raft formation and stability, membrane fusions an membrane trafficking.[2, 3]

As stated, flat lipid bilayers under periodic boundary conditions provide a simple and effective model system for biological membranes. Nonetheless, in order to avoid size effects[1], the simulations of a hydrated bilayer at the atomistic level requires a number of atoms in the order, at least, of tens of thousands, resulting in a high wall-time even resorting to efficient parallel algorithms such the as the domain decomposition method (DDM).[4, 5, 6]

Typically, on the CRESCO3 HPC platform[7] a relatively small system, such as a hydrated lipid bilayer of 36 molecules of palmitoyl oleoyl phosphatidylcholine (POPC) per leafleat ( about 17000 atoms), can run with a maximum speed of 20-25 nanosecond per day using the popular GROMACS Molecular Dynamics (MD) program[8, 5] exploiting at most 160 processors with an efficiency of less than 50%. This is so since, after a certain processor number, the inter-domain communication overhead dominates over the time spent in the computation of the forces within each domain. In other words, in DDM schemes there is an *optimal domain size* (ODS/DDM) for a given HPC configuration. The ODS/DDM is in the order of few hundreds atoms on most of the common CPU-based or GPU-based HPC architectures.[9]

The saturation problem on parallel platform can be obviously circumvented by simply increasing the size of the sample, i.e. by increasing the number of ODS domains to be assigned to each processor. In this way, the

simulation speed in terms of ns/day remains roughly independent on the size of sample, provided that number of available cores is equal to or greater than the number of ODS domains. If, on one hand, large samples allow, by taming fluctuations of ensemble averages, a faster convergence of key static membrane properties such as mean lipid area, head-to-head thickness, bending rigidity and undulation spectra, a wider surface requires longer traveling times for a diffusing component thus increasing significantly the equilibration times for, e.g., perfect mixing of a two component system under scrutiny.[10] The transport problem is so acute in the membrane simulation practice, that, trading model accuracy in exchange for computational speed, approaches have been developed using the *coarse-grained* models, where larger molecular units are considered as single particles.[11]

In this report we investigate on the effectiveness of using advanced Hamiltonian Replica exchange schemes (HREM) with selective scaling of specific degrees of freedom of the system[12, 13, 14, 15, 16] as a mean for boosting configurational sampling in simulations of model membranes at the atomistic level. Enhanced sampling techniques for membrane simulations has been recently reviewed by Mori *et al.*[17]. Standard temperature REM in membrane systems has the obvious drawback that the simulation must be performed in conditions of *constant volume*, in order to preserve the integrity of the system and avoid catastrophic behavior at high temperatures. While it has been recognized[18, 19] that the existence of sharp cooperative transitions (such as phase transitions) can lead to temperature exchange bottlenecks in REM schemes and significantly reduce the sampling efficiency, nonetheless standard temperature REM methods have been recently used as an expedient to gain insights on the sol-gel transition in coarse grained lipid bilayer models as a function of temperature in conditions of constant pressure, pushing the upper temperature limit (390 K) slightly beyond the water boiling point.[20] Enhanced sampling techniques has been employed to study the conformational landscape of proteins embedded in biological membranes[21, 22] To our knowledge, the only *genuine* replica exchange scheme (i.e. a simulation scheme for *enhanced sampling* of a target thermodynamic state) of a membrane bilayer system to date was proposed by Mori *et al.*[23] in the context of NP$\gamma$T simulations. Their generalized ensemble (GE) approach is based on exchanges between few replicas spanning the surface tension ($\gamma$) space, rather than the temperature space, from zero tension of the target replica to higher tensions, obtaining a moderate gain in the convergence time of structural parameters.

On the other hand, recent studies have highlighted the key importance of lipid flexibility and entanglement in shaping the transport and undulation phenomena in biological membranes.[24, 3]. These molecular properties, in turn, have time scale dynamics that are essentially dictated by the free energy barriers separating *gauche* and *trans* states for the dihedral conformation of the torsion around the $sp^3$ bonds of the alkyl chains in the hydrophobic interior of the bilayer. One can hence infer that, by selectively scaling, along the replica progression, the energy terms implied in these barriers (i.e. dihedral potentials and 1-4 Coulomb and Lennard-Jones interactions), the jump rate for *gauche trans* interconversion can be exponentially increased in the hot replicas, thereby enhancing diffusion and area/volume modulation throughout the GE, in condition of *constant pressure*, without necessarily triggering phase transitions due to the fact that most of the degrees of freedom of the system remain at the target temperature. Along precisely this line of reasoning, a biased torsional potential with user adjustable parameters, for example, has been recently used to boost conformational sampling in the lipid phase by McCammon and coworkers without observing catastrophic cooperative phenomena.[24, 25] Their approach, termed "accelerated MD" (aMD), is actually equivalent to a single standard Umbrella Sampling simulation[26] with a torsional bias potential and, while useful for speeding up diffusion and conformational sampling, has the well known limitations in the acquisition of the average properties due to the high energetic noise produced by the bias potential when re-weighting back to the unbiased system.[17]

In this paper we shall describe and test on a POPC atomistic-level bilayer system, a rigorous, parameter free, torsional tempering scheme in the context of a genuine replica exchange simulation, allowing to collect, in few ns or tens of ns time span on the target state, a manifold of equilibrium configurations statistically out of the reach of conventional (single trajectory) simulations. The present report is organized as follows. In the Section *Theoretical background*, we briefly summarize the theoretical aspects of the HREM technique, with emphasis on torsional tempering for membrane simulations. In the *Methods* section, we succinctly describe the system and the various parallel simulation techniques used in our contribution. In the section *Results*, we compare configurational properties such as volume and area fluctuations, diffusion and bilayer structure obtained using the HREM approach as opposed to the conventional single trajectory technique. In the *Conclusions* Section conclusive remarks are presented.

## 2. Theoretical background

*2.1. Hamiltonian Replica Exchange and Solute Tempering schemes*

"Solute tempering" was introduced originally by Liu and Berne.[27] These authors developed a variant of the temperature replica exchange method (T-REM) whereby the solvent-solvent interaction energy is rescaled along the replica progression such that it vanishes in the exchange probability. This partition was strictly defined for the "real" solvent. In the Hamiltonian Replica exchange method[12, 13], rather than globally scaling the temperature of the system as in T-REM, each state in the generalized ensemble is characterized by its own potential energy function. A flexible and efficient solute tempering scheme has been recently formalized[15] in the context of HREM. This approach relies on the definition of independent scaling factors for each of additive components of the total potential energy of the system. Following Ref. [15], the potential energy function of the $m$-state in HREM can hence be compactly written as

$$V_m(X) = \mathbf{c}_m \cdot \mathbf{V}(X) \tag{1}$$

where X represent a configuration of the system and where the components of the vector $\mathbf{V}(X)$ correspond to the individual additive terms in the system potential energy, i.e. $V(X) = \sum_i V_i(X)$. The $\mathbf{c}_m$ vector is the scaling vector for state $m$, where the $i$-th component is the scaling factor in the $m$ state for the $V_i(X)$ additive term. In the target (unscaled) state, all the components of the $\mathbf{c}$ vector are equal to 1, so that $V_m(X) = V(X)$. The transition probability in a replica exchange scheme with the state potential energy given by Eq. 1 is given by

$$P = \min(1, e^{\beta \Delta \mathbf{c} \Delta \mathbf{V}}) \tag{2}$$

with $\Delta\mathbf{c} = \mathbf{c}_{m+1} - \mathbf{c}_m$ and $\Delta\mathbf{V} = \mathbf{V}(X_{m+1}) - \mathbf{V}(X_m)$. From Eq. 2, it is easy to see that only the potential terms $V_i$ that are scaled (i.e. those corresponding to components $c_m^{(i)} \neq 1$) will affect the exchange probability. Also note that all replicas are simulated at the same inverse temperature $\beta$ and when all components of the $\mathbf{c}$ vector are scaled coherently (i.e $V_m = c_m V$), one recovers the standard Hamiltonian REM with the scalar scaling factor $\beta c_m$ playing the role of a scaled inverse temperature.

With this powerful formalism, in a single accepted replica exchange event, the vector $\mathbf{c}$ can be swapped instead of the coordinates (thereby keeping, as in

T-REM, the communication overhead at a nominal level) and local scaling can be implemented in a very general fashion using an appropriate, user defined partition of the system and/or of the potential function $V(x)$. By limiting the scaling to selected portions of the overall potential energy, the system can be surgically heated on few relevant degrees of freedom, therefore limiting the number of replicas in the GE also when implementing a very small scaling factor $c$ corresponding to very high local temperature $T/c$.

In a solute tempering scheme, for example, the "solute" and the "solvent" are by definition the part of the system which will be scaled and the unchanged part, respectively. In HREM implementations based on Eq. 1[28, 29, 30, 31, 32], any subset of atoms out of the N system atoms can be selected, thus defining the solute. This subset may include disconnected portions of real solute, as well as selected solvent molecules. The scaling factor $c$ for the additive component of the so defined "solute"-"solvent" potential can be chosen at will and can involve different contribution of solute, solvent or solvent-solute potential. In the EDU-REM implementation (Energy Driven Undocking Replica Exchange Method), for example, solute-solvent interactions were *counterscaled* (i.e. the corresponding $c$ component was increased along the replica progression) to favor the extrusion of the ligand from binding pocket by increasing the hydrophilicity of the ligand and of the binding site.[32] Along similar lines, Oleinikovas *et al.* implemented a variant of the HREM, called SWISH-HREM[33], relying basically on an progressive alteration of the non bonded interaction between water and surface protein atoms along the GE using a single scaling parameter $\lambda_m$ so as to render water more ligand-like in the hot replicas with the final aim of identifying cryptic pocket in the apo protein.

We finally must mention the fact that an even more general and flexible HREM approach with respect to that based on Eq. 1 has been recently implemented in the powerful MD plugin PLUMED[34, 35] whereby each replica is fed its own GE state topology/parameter file, swapping coordinates between neighboring replicas rather than scaling factors as in Ref. [15]

### *2.2. Torsional tempering for membrane simulations*

The potential energy function in solvated lipid bilayers is given by a sum of additive terms of the kind

$$V = V_{\text{Bonded}} + V_{\text{Nbonded}} + V_{\text{tors}} \tag{3}$$

where $V_{\text{Bonded}}$ includes the stretching and bending potential terms, the term $V_{\text{Nbonded}}$ refers to the electrostatic and Van der Waals interactions between non bonded atoms of the solvent, of the lipidic phase, and the mixed term due to the lidip-water interactions. $V_{\text{tors}}$, finally, is the dihedral potential that concerns only the lipidic phase. In order to boost *gauche-trans* conformational transitions in the lipid bilayer, a straightforward partition in a HREM is implemented as follows:

$$V_m = V_{\text{Bonded}} + V_{\text{Nbonded}} + c_m V_{\text{tors}} \tag{4}$$

whereby all the component of the **c** vector are 1 except for that referring to the dihedral energy $V_{\text{tors}}$. Note that $V_{\text{tors}}$ includes also the 14 non bonded interaction terms. In this fashion, the exchange probability, Eq. 2, depends only of the energy difference $\Delta V_{\text{tors}}$ between neighboring replicas, i.e $P = \min(1, e^{\beta \Delta c \Delta V_{\text{tors}}})$. The scheme used in Eq. 4 may be viewed as lipid torsional tempering where only the lipid dihedral angles are heated along the replica progression while all other degrees of freedom remain cold.

Given this HREM partition, the optimal scaling protocol must evidently result from a compromise between the choice of the largest possible scaling factor (that guarantees an easy *gauche-trans* barrier crossing in the lipid phase) and the minimal number of replicas that is needed to span the energetic GE space, with a spacing tuned so as to have a constant acceptance ratio along the replica progression. In other words, the only free parameter of this HREM approach is the maximum allowed torsional temperature, $T_t^{(max)} = T/c_{min}$, in the GE.

## 3. Method

### *3.1. POPC simulation setup*

The simulations of the lipid bilayer, whether conventional or in the GE, comprised 72 POPC lipid units (36 for leaflet) with approximately 30 water molecules per lipid. The total number of atoms in the system was 16374. The starting PDB configuration was an equilibrated charmm36 configuration, downloaded from ref. [36]. The force field employed is a minor modification[37] of the most recent update of AMBER/GAFF[38] compatible parameters for lipids by Jämbeck et al., called *Slipids*, recently developed for fully saturated phospholipids.[39] All the simulations - both conventional and GE - were performed in the isothermal-isobaric ensemble, NPT, at an

external pressure of 0.1 MPa. The pressure was held constant by a Parrinello-Rahman barostat [40], with a 70 $cm^{-1}$ oscillator frequency and compressibility set to $5.3 \times 10^{-4} MPa^{-1}$ and semi-isotropic stress. The temperature was held at 303 $K$ by means of a Nosé-Hoover thermostat.[41, 42] Electrostatic interactions were treated using Particle Mesh Ewald[43] with a b-spline order parameter of 4 and a grid spacing of 1.2 Å. The TIP3P water model [44] was used. The switch-off of Lennard-Jones interactions was set at 13 Å, with no long-range correction. Constraints were imposed only on bond involving hydrogen atoms.

*3.2. HREM simulation setup*

The HREM scheme is based on the torsional scaling defined in Eq. 4. We used $N_r = 24$ replicas in the GE with a scaling factor ranging from $c_1 = 1$ (target state, no scaling) to $c_{N_r} = 0.3$ (corresponding to a "torsional" temperature of 1010 K for the hottest replica). In order to further reduce the number of degrees of freedom involved in the scaling, thus reducing the number of replicas needed to span the given energy scale in the GE, we choose to include in the definition of "lipid" only a part of the molecule, i.e. that involving hydrophobic chains, as shown in Figure 1, given that the scaling of the dihedral appears to have a rather modest effect on the conformational sampling rate of the solvent exposed head-groups. The replica spacing was tuned by trial and errors on short (0.4 ns ) simulations of the system. An optimal scaling, yielding an approximately constant acceptance ratio of about 13% in the GE, was obtained as an arithmetic mean between the standard geometrical progression[12] and a simple linear scaling i.e.

$$c_m = \frac{1}{2}\left( c_m^{\frac{(m-1)}{(N_r-1)}} + \frac{c_{N_r}-1}{N_r-1} m + \frac{N_r - c_{N_r}}{N_r - 1} \right) \tag{5}$$

The replica exchange frequency was set[45] to about 30 $ps^{-1}$ (exchange were attempted every 36 fs) yielding an average of 2 accepted moves per picosecond.

In Figure 2 we show the effect of the outlined torsional scaling on the *gauche-trans* distribution in the lipidic phase of a POPC bilayer. In the left panel we show the full torsional energy around a single C-C bond for the target state with scaling factor $c_1 = 1$ and for the highest replica (scaling $c_{24} = 0.3$). In the right panel of Figure 2, we report the dihedral angle distributions for the aliphatic torsion angles of the lipid chains in the GE and,

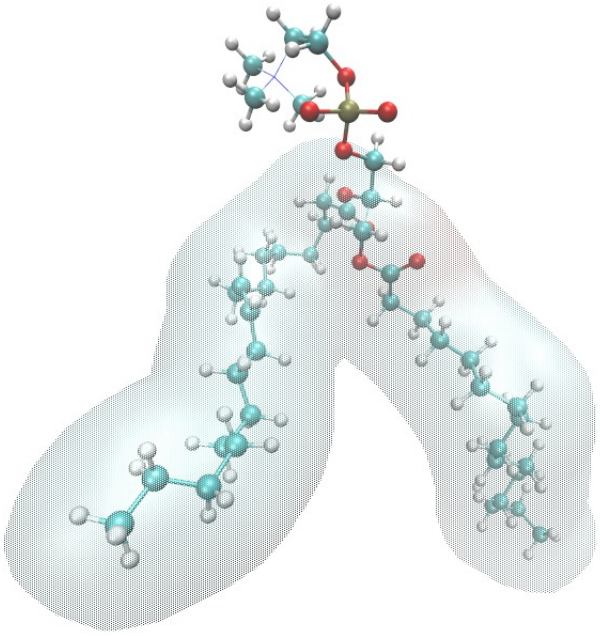

Figure 1: The torsional scaling protocol, Eq. 4, applies only to dihedral angles and corresponding 14 interactions involving the highlighted atoms in a POPC lipidic unit

in the inset, the jump rate of a single bond between *gauche* and *trans* states as a function of the GE state index $m$. These properties were determined by performing a 180 ps simulation on each of the GE state using the above defined scaling protocol and by averaging on all torsion angles of the alkyl chains of the lipids. As expected, the free energy barrier between *gauche* and *trans* states steadily decreases along the replica progression with the jump rate being consequentially boosted exponentially with increasing scaling. In the target state ($c = 1$) each single C-C bond experiences on the average around 10 *gauche-trans* conversions per nanosecond. In the hottest torsional state ($c = 0.3$) the mean jump rate on a single bond skyrockets up to about

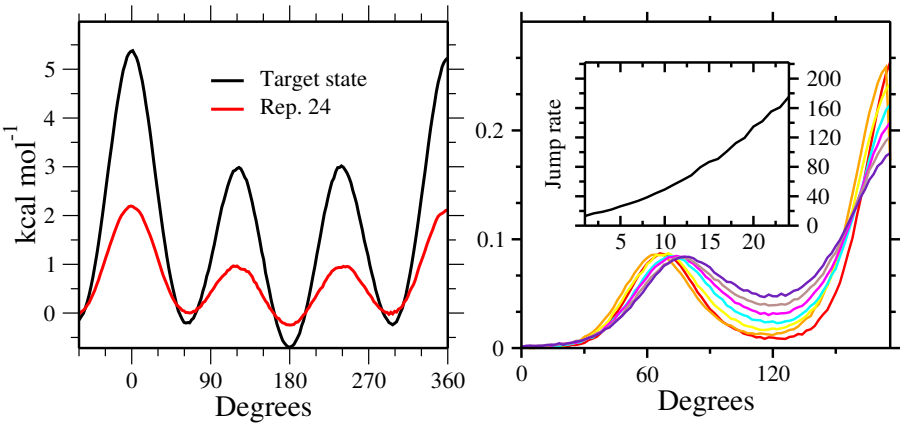


Figure 2: Left: torsional energy round the internal aliphatic C-C bond (Jämbeck type `a3`, see Ref. [39]); black trait, target replica; red trait, hottest replica. Right: probability distributions of the dihedral angle averaged on all aliphatic torsion angles in a non exchanging 1 ns GE simulation. Color coded scheme for distributions: from red (target state) to violet (hottest torsional state). In the inset, the jump rate per ns is reported as a function of the scaled state.

160 *gauche-trans* conversions per nanoseconds.

### *3.3. Parallel protocol used on HPC for conventional and HREM simulations*

The conventional simulation of POPC bilayer was performed using the GROMACS program.[46] Since stretching involving non hydrogen atoms were not constrained, equations of motion were integrated with a time step of 1 fs in order to avoid artifacts due to non accurate numerical integration. In

Table 1: Performances of the GROMACS code (version 4.6, compiled with Intel-FORTRAN ) on the POPC system (16374 atoms). Measures were done on the ENEA-grid CRESCO3 HPC platform. The ODS for lipid bilayer in standard condition is indicated in bold.

| Nprocs. | Speed (ns/day) | efficiency | Domain size |
|---|---|---|---|
| 1 | 0.27 | 1 | 16347 |
| 32 | 8.37 | 0.96 | 511 |
| 64 | 14.85 | 0.85 | 255 |
| 96 | 19.296 | 0.74 | **170**(ODS) |
| 160 | 20.900 | 0.48 | 102 |

Table 1 we show the speed up ratio obtained on the POPC system with GROMACS on CRESCO3, a European Tier-2 HPC form equipped with 24-cores AMD Opteron 6234 processors. As stated in the introduction, due to the ODS/DDM restraint, the moderate size of the system (about 17000 atoms) allows to run with a *maximum* speed of 20-21 ns per day on CRESCO3 using at most 160 processors with an efficiency of less than 50%. The threshold speed for a program investing all resources in the parallelization of the forces using DDM is in essence dictated by the ODS, that is, the size of the domain, applied to condensed phases in standard conditions, for which efficiency loss due to the inter-domain communication overhead is less than 25%. On high-end architectures with high speed InfiniBand connection, the ODS is hence weakly dependent on both the CPU design and the size of the system. So, on CRESCO3 we can run with an efficiency of 75% a POPC system with 17000 atoms ( corresponding to 6x6 lipids layer with side-length of about 5 nm) at a maximum speed of 20 ns/day *circa*. Using the full dedicated CRESCO3 cluster (2016 cores) and assuming no efficiency loss, one can perform a simulation of a system made of about 400000 atoms (corresponding 28x28 lipids layer of side-length of about 22 nm) at the same speed of 20 ns/day. It follows that for the conventional (DDM-based ) parallel approaches running on standard low latency/high bandwidth communication systems, the threshold simulation speed for the POPC system is in first instance a function of the core clock speed only. Actually, when increasing the size of the simulated system, due care must be taken for preserving the neighboring relationship between communicating processors via Dynamic Load Balancing[47], since breaking of neighboring relationship among the processors/domains, leading to irregular communication patterns, may increase significantly the communication overhead. On the European Tier-0 resource Marconi provided by CINECA consortium[48] (Italy), mounting the Intel-Xeon Broadwell CPUs (whose core unit is from 4 to 5 times faster than the CRESCO3 AMD Opteron core for the MD force loop), the maximum speed for the POPC system with the simulation set-up previously described, can be forecasted not to exceed 100-120 ns/day using GROMACS.[8] This is indeed a severe limitation for conventional DDM-based simulations, since even with the availability of thousand of cores, as it normally happens on modern HPC platforms, one is forced to increase the size of the system to enhance the statistics for static properties. This strategy, on the other hand, is counterproductive when mixing of multicomponent system is at stake.[10] In the present study, we choose to run two independent 96 processors conventional simulations of the 17000

atoms POPC system each lasting 100 ns, investing a total of about 23000 core hours.

The GE simulations were performed using the ORAC program[15, 49] on the CRESCO3 HPC facility.[7] ORAC is an hybrid OpenMP/MPI code with a flexible allocation of parallel resources, specifically tailored for Non Uniform Memory Access (NUMA), CPU-based HPC facilities. We run two GE simulations of the POPC system each producing about 50 nanoseconds on the target state and 1 $\mu s$ of simulation in total. These simulation required in the order of 80000 core hours, each. In first instance (HREM-5x10), exploiting the `battery` option in ORAC, in a single parallel job, we run for 5.5 ns 10 independent sets of 24 GE replica walkers, for a total of 240 MPI parallel processes. In this HREM-5x10 simulation, the Hamiltonian scaling protocol is identical for each of the ten 24-walkers sets and all parallel resources are dedicated to the weak scaling algorithm for the production of the 240 GE trajectories. For the production run, MPI communication groups are defined only within each of the 24-walkers batteries, accumulating statistics *vertically* for a total of 55.0 ns on the target state. Each of the 240 MPI instances, corresponding to the exchanging simulations in the GE, are numerically integrated on a single core using an efficient multiple time step setup[50, 51], running at a speed of 0.4-0.5 ns/ day on the CRESCO3 platform. The parallel efficiency of HREM-5x10 is basically linear, hitting 97% at 240 processors and showing no significant sign of degradation up to 384 processors.

| | DDM | HREM-5x10 | HREM-50x1 |
|---|---|---|---|
| core hours x1000 | 23 | 79 | 86 |
| Total simulation time ($\mu$s ) | 0.2 | 1.3 | 1.2 |
| Target state simulation time (ns) | 200 | 55 | 50 |
| total number of parallel instances | 96 | 240 | 192 |
| MPI processes | 96 | 240 | 24 |
| NTHREADS(OpenMP) | 1 | 1 | 8 |
| overall parallel efficiency | 0.75 | 0.97 | 0.75 |

Table 2: Simulation protocols on the CRESCO3 HPC system (CPU unit: 24-cores AMD Opteron 6234) for conventional simulation (DDM), multibatteries GE simulation (HREM-5x10) and hybrid OpenMP/MPI GE simulation (HREM-50x1)

In a second GE simulation (HREM-50x1) we run a single set of 24-replica GE simulation for 50 nanosecond using an hybrid OpenMP/MPI parallel approach, hence *horizontally* accumulating statistics on the target state. Each

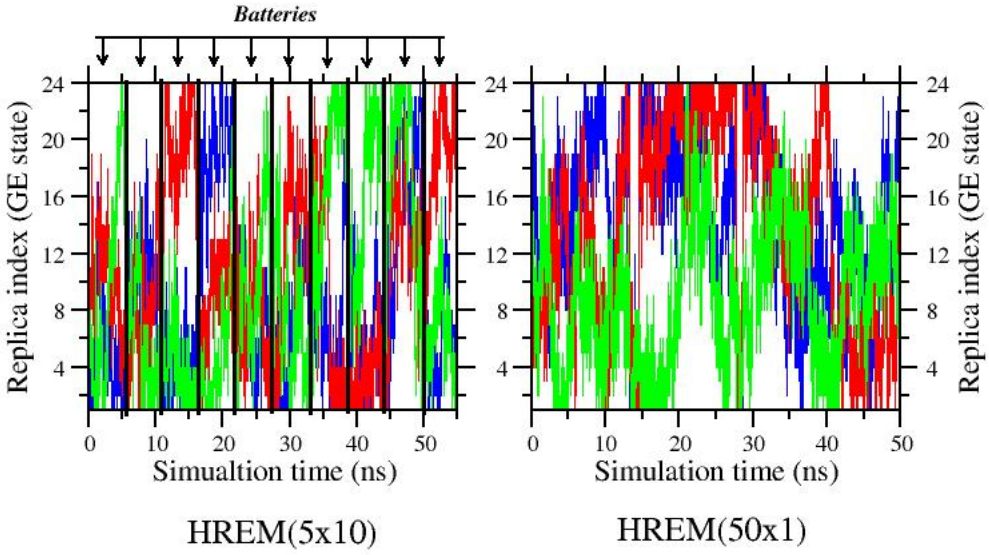


Figure 3: Time record of the replica index in the HREM-5x10 and HREM-50x1) simulations. Only three GE walkers out of 24 are shown.

MPI instance or trajectory used in this case 8 threads on the OpenMP layer, the full hybrid job engaging a total of 192 cores. In this case the efficiency loss is of 25% and is entirely due to the high communication overhead on the ORAC OpenMP layer enforced via a shared memory force decomposition scheme.[49]

In HREM simulations, in order to minimize the communication overhead, the GE index and corresponding scaling factors are exchanged rather than configurations. In this way, each trajectory (or walker) spans the entire GE space with ideally uniform probability and time-ordering of a single GE states must be done *a posteriori*. In Figure 3, we show the time record of the GE state index in three typical exchanging trajectories taken from the HREM-5x10 and HREM-50x1 simulations. In case of the HREM-5x10, the 10 independent HREM simulations have been lumped together producing an overall of 55 ns sampling per GE state, with the simulations of the individual batteries being delimited by vertical black lines. As seen on the left panel in Figure 3, while round-trips are rarely seen in a single battery 5.5 ns simulation, the round-trips are easily attained when joining all 10 independent runs in the full 55 ns time span and the diffusion pattern of the replica index of

HREM-5x10 is similar to that of the single battery HREM-50x1 simulation so that both parallel protocols are expected to produce similar enhanced sampling effects on the target state. Finally, the replica diffusion in both simulations shows apparently no sign of bottleneck, thus indicating that the adopted torsional scaling protocol does not involve major collective transformations of the lipidic bilayer which remains fluid throughout the entire GE. Salient data about the parallel protocol and performances for the the conventional DDM simulation and for the two GE simulations are collected in Table 2.

Beside the benefits due to the enhanced sampling (see the Results section further on), as long as static properties and lateral lipid diffusion are concerned, in the two HREM simulations, in principle, by means of the so-called Multistate Bennett Acceptance Ratio (MBAR) re-weighting scheme,[52, 53] one can use the statistics collected from the all replicas for a total simulation time of 1 $\mu$ $s$, i.e. ten times more than that acquired during the two conventional 100 ns simulations. The MBAR weights of all configurations in the GE can be straightforwardly computed keeping track of the unscaled torsional potential energy.[53] It must be pointed out, however, that the mean weights of the $m$-th GE configurations at the target (unscaled) state decrease exponentially with the difference between the corresponding average torsional potential energies. In our 24 states simulations, while the MBAR weights of the target state configurations are basically unitary, those of the *second* GE state, i.e. that contributing the most to the target state properties, are already so small (in the order of $10^{-3}$ ) that their contribution to the averages in the target state can be assumed to be negligible. In the Results section, all the averages were calculated using configurations sampled in the target state only.

## 4. Results

In this section we shall assess the effect of torsional tempering in GE HREM simulations on key properties of biological membranes, i.e area and volume per lipid, bilayer thickness and lipid diffusion. In Figure 4, we show the time record of the area per lipid of the HREM-5x10 simulation and of the conventional DDM simulation on the POPC system. Lipid area fluctuations are important for the determination of the bending rigidity of the membrane in the continuum (low wavelength) limit, while lipid lateral diffusion determines the mixing rate and equilibration of in-homogeneous systems. In

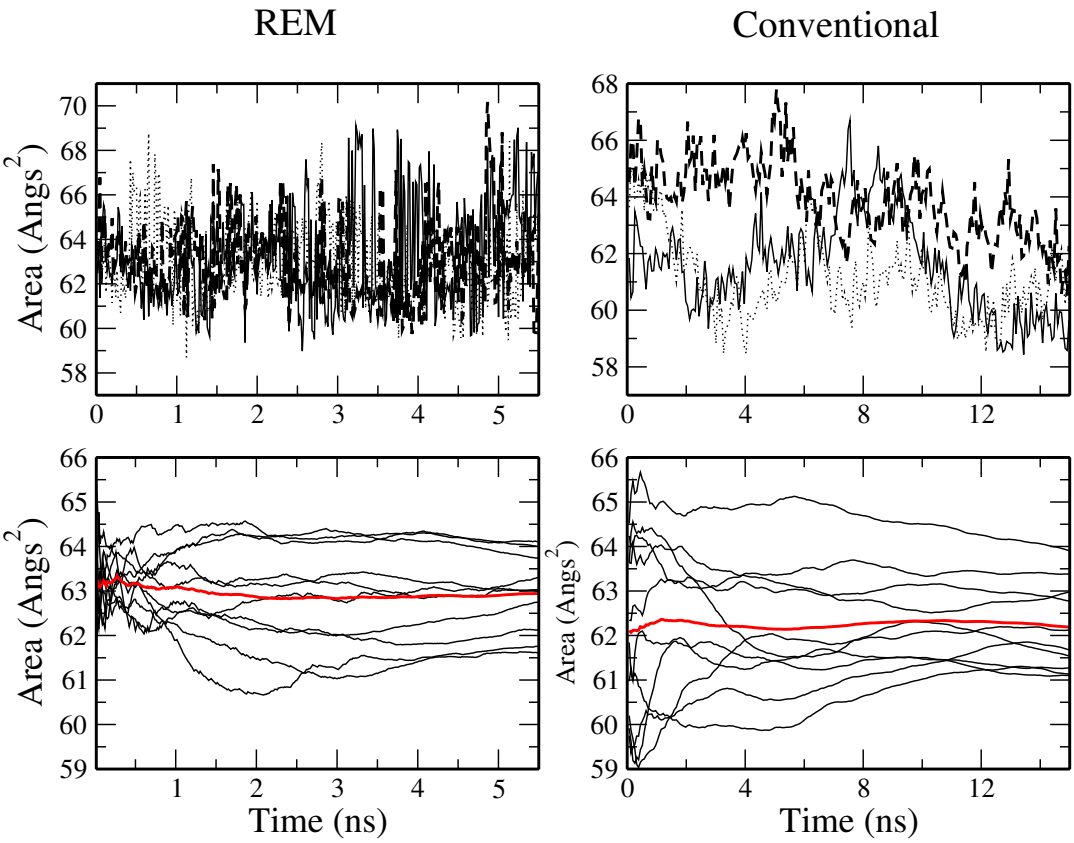


Figure 4: Top: Time record of the area per lipids in HREM and conventional simulations at T=303 K. The time record of only three 5.5 ns HREM batteries (target states) and three 15 ns conventional sub-simulations are shown for clarity. Bottom: Area per lipid running averages evaluated in HREM for each of the 10 batteries target states and for the conventional simulation in 15 ns time span taken from two independent 100 ns simulations. The red curve is the cumulative running average over ten 5.5 batteries (REM) and on 200 ns of conventional simulation

HREM-5x10, the average area over all 10 target states configurations in 5.5 ns appears to have reached a stationary value. Given the variance of the running averages recorded in each of the ten independent batteries, a more accurate results can be straightforwardly attained by simply increasing the number of the independent HREM simulations of course engaging more computational resources, if available, but *with no impact whatsoever on the wall-clock time*. In the HREM-5x10 simulation, in spite of the short simulation time span

(only 5.5ns), the fluctuations of the area undergo a clear boost from the GE exchanges, exhibiting variations up to 8 Å$^2$ in a time as small as the fraction of the picosecond. This is so since the average area per lipid of the hot GE states is sensibly larger than that of the target state increasing up to about 66 Å$^2$ in the last GE state. These large area states are transmitted, within a single battery, in few or few tens of picoseconds through the exchanges in the target replica with the correct Boltzmann weight. The conventional simulation, reported on the right in Figure 4, shows in general much smaller area fluctuations with respect to HREM-5x10 in the short time scale. Larger fluctuations can only be observed in the super-nanosecond timescale, making difficult the acquisition of a stationary value of the mean and standard deviation of the area in a 100 ns time span.

In Figure 5 we compare the time record of the area (left) and volume (right) per lipid for the HREM-50x1 simulation at the target state and as a function of the replica index (in the insets). The HREM-50x1 single battery simulation, due to the low number of OpenMP threads for each of the 24 trajectories (see Table 2), required a wall clock time that was only slightly longer than that of the HREM-5x10 10 batteries simulations. Results for the HREM-50x1 50 ns run, as far as mean lipid area and fluctuations, are very similar to those shown in Figure 4 referring to the short 5.5 ns HREM-5x10 and to the 200 ns conventional DDM simulations. In Figure 5 we also report (see the insets) the running averages of the lipid area and volume for some selected GE states using a color-code for the corresponding torsional temperature. Expectedly, the area per lipid, $A_L$ steadily increases with increasing torsional temperature in the GE, while the lipid volume, $V_L$, decreases. This opposite trend of area and volume is reflected by a steadily decreasing thickness of the layer as we climb along the GE scale. The mean layer thickness, defined as $t = 2V_L/A_L$, goes from 40.4 Å in the target state to 37.9 Å in the hottest replica. These value are indeed reminiscent[54] of the trends observed in experimentally measured bilayer area and thickness for temperature ranges in the order of the 300-350 K, implying that the hottest torsionally tempered GE state at $T_t = 1010$ K in the GE simulation behaves essentially as fluid phase at the real temperature of T=80$^o$.[54]

In Table 3 we collect the results obtained with the HREM-5x10 simulation, with replica generation done on the MPI layer only, the HREM-50x1 simulation that uses an hybrid parallel algorithm OpenMP/MPI, and finally the conventional 2x100 ns DDM simulations. The three methods appears to yield in essence the same physical picture of the POPC system, as long as

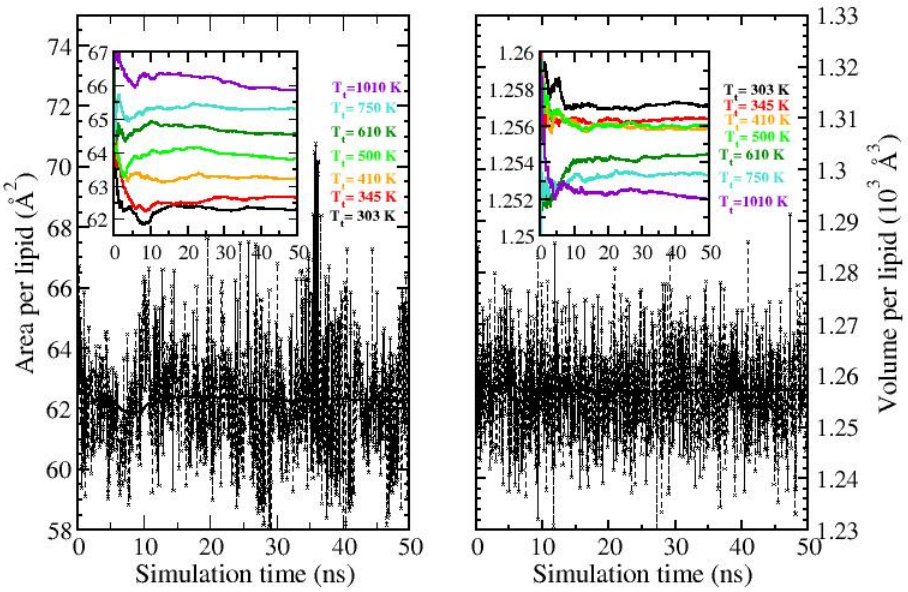


Figure 5: Left: Time record of the area (left) and volume (right) per lipid in the single battery 50 ns HREM-50x1 simulation on the (time-ordered) target state. The solid black lines corresponds to the running averages. In the insets we report the running averages of the area and volume per lipid for some selected time ordered GE states. The corresponding "torsional" temperatures are shown from the coldest (target) state ( $m = 1$ $T_t = 303$ K, black trait), to the hottest state ($m = 24$ $T_t = 1010$ K, violet trait)

average lipid area and volume are concerned. For conventional simulations, errors were computed by block averages on 15 ns segments. For HREM-5x10 errors were computed by averaging over the target states sampled by the 10 independent GE batteries. For HREM-50x1, finally, errors were assessed by block bootstrapping on samples containing 1/20 of the total sampled configurations on the target state.

In Figure 6 (left) we show the undulation spectrum[57] of the POPC system for HREM and conventional simulation. We used the coordinates $z$ coordinates of the phosphorous atoms on the two leaflets to define the undulation function $u(x, y) = \frac{1}{2}(z_1(x, y) + z_2(x, y))$ and the local thickness

| | $A_L$ | $V_L$ | $K_A$ | $D_{HH}$ | G/T ratio |
|---|---|---|---|---|---|
| **HREM-5x10** | 62.9±1.2 | 1262.0±0.8 | 164±40 | 38.4 ±0.1 | 0.261 |
| **HREM-50x1** | 62.2±0.2 | 1257.0±0.6 | 381±35 | 37.6 ±0.1 | 0.264 |
| **Standard MD** | 62.2±1.3 | 1247.7±1.3 | 388±65 | 39.0 ±0.2 | 0.260 |
| **Experiments** | 64.3[a]±1.3 | 1256[b] | 180-330[c] | 36.7 [a] | - |

Table 3: Area per lipid ($A_L$ in Å$^3$ units), volume per lipid ($V_L$ in Å$^3$ units), isothermal area compressibility modulus ($K_A$ in $10^{-3}Nm^{-1}$ units), bilayer thickness ($D_{HH}$ in Å) and *Gauche/Trans* ratio from POPC HREM simulation, standard MD simulation and experiments: **a.** from ref. [54] **b.** from ref. [55] **c.** from ref. [56]

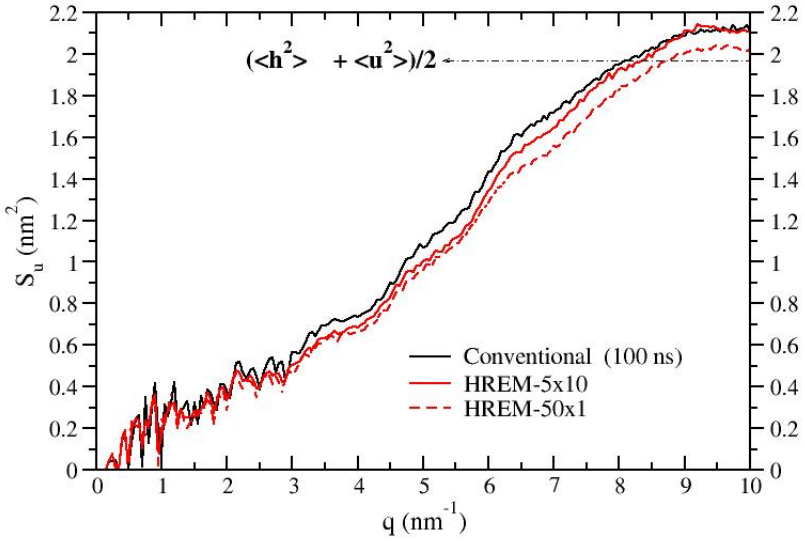


Figure 6: Fourier transform of the membrane undulation function[57] $u(x,y) = \frac{1}{2}[z_1(x,y) + z_2(x,y)]$.

$h(x,y) = \frac{1}{2}(z_1(x,y) - z_2(x,y))$. In this case, the local thickness can approximately be related to one half of the $D_{HH}$ thickness, defining the distance between the maxima in the electron density profile.[55] Inspection to Figure 6 shows that conventional and HREM simulations yield similar results,

exhibiting similar trends and approximately the same limiting value at long wavelength. Due to the moderate size of the sample, the $q^4$ short wavelength behavior[57, 3] could not be observed.

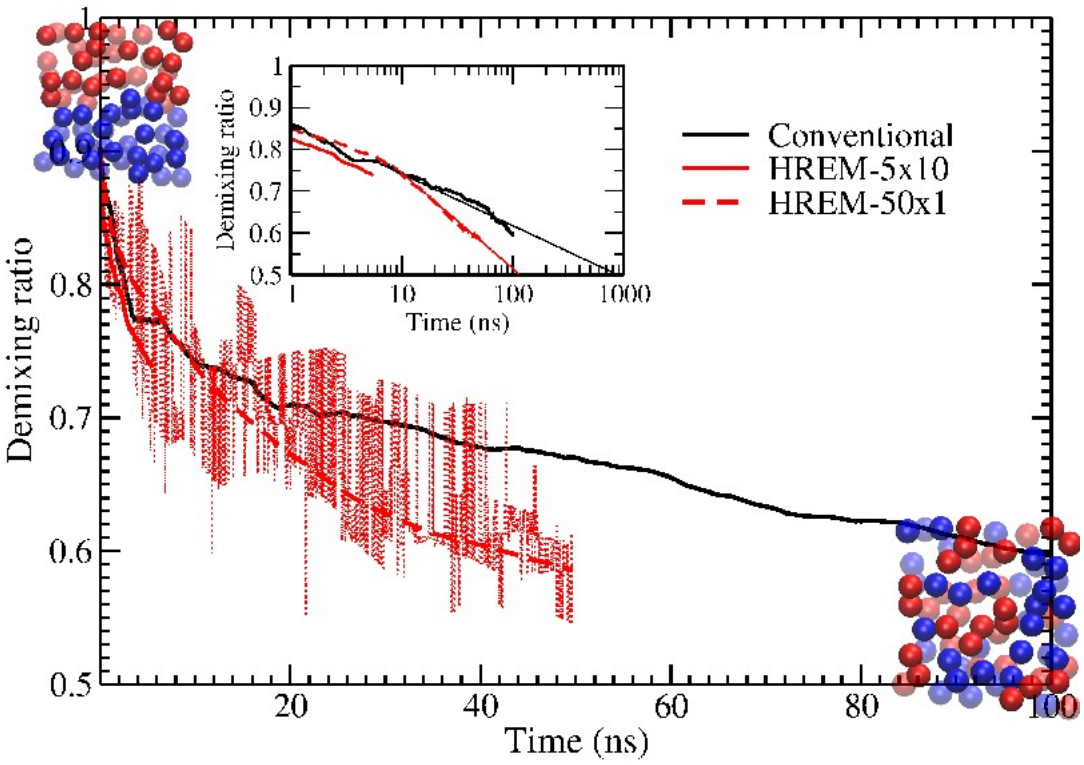


Figure 7: Time record of the mixing probability. For the HREM-50x1 data (red curve) the demixing index $D(t)$ was averaged over all 10 GE target states. For the HREM-50x1 simulation (heavy dashed red line) we report the GE averaged $D(t)$. The thin dashed red line corresponds to the time record of $D(t)$ for the target state only of the HREM-50x1 simulation. In the inset, the same plot is reported on a logarithmic scale. The thin black and red lines are the result of a linear fit on conventional and GE data, using the last 50 and 25 ns, respectively

In Figure 7, finally, we show the mixing functions for the GE simulations HREM-5x10and HREM-50x1 and for the conventional simulations, obtained by labeling at the start of the run ($t = 0$) with two different colors two identical sets of phosphorous atoms based on their t=0 y-coordinate. This labeling defines the demixed zero time state, showed in the upper left corner of the plot. We then define the demixing index $D(t)$, as the probability of

a phosphorous atom to have the nearest neighbor bearing the same label (or color) as the simulation proceeds. In the starting state, such probability simply reflects the impact of the ideal linear boundary separating the labeled particles on the layer surface. As the 2D size grows, D(0) tends to unity while $\lim_{t\to\infty} D(t) = 0.5$ for a perfectly mixed state irrespective of the sample size. The thick red line for HREM-5x10 has been obtained by averaging $D(t)$ over the ten batteries of target state configurations. In the HREM-50x1 simulations, because of the exchanges, the time ordered trajectories on all GE states yield comparable probability evolution and hence one can define a time dependent probability of demixing averaged over the whole GE ensemble (thick dashed line). Note that the extremely irregular behavior of the target state evolution of $D(t)$ in HREM-50x1 (thin red line, main plot) is due to replica exchanges. Both HREM protocols produce indeed a significant acceleration of mixing with respect to the conventional simulation, especially evident in the inset logarithmic plot. This GE-induced mixing enhancement is moderate in the 5.5 ns HREM-5x10 simulation as an increase of lipid lateral diffusion can occur only via the *indirect* effect of enhanced torsional *gauche-trans* switching across the GE while all other degrees of freedom remain cold. On the other hand, while at 100 ns the conventional simulation exhibits a $D$ index of about 0.6, the HREM-50x1 simulation shows nearly perfect mixed configurations of the target state starting as early as 20 ns (see the thin dashed line in Figure 7). Perfect mixing can be roughly estimated to occur in our sample between 0.5:1 $\mu$s for conventional simulation and at about 0.1 $\mu$s for the HREM-50x1 simulation with a gain of 1 order of magnitude in mixing speed due to GE enhanced sampling.

## 5. Conclusions

We have devised a Hamiltonian Replica Exchange protocol with torsional tempering scheme, specifically tailored for the molecular dynamics simulation of model biological membranes on massively parallel platforms. The proposed HREM scheme, carefully tuned for atomistic model biological membranes, involves only a small faction of the degrees of freedom of the system, therefore keeping, at the same time, the number of exchanging replica states small and allowing large scaling factors for the torsional potential in the lipidic phase.

By comparing the results of the runs obtained using vertical (HREM-5x10) or horizontal (HREM-5-x1) parallel schemes, we have shown that HREM jobs can produce in few nanoseconds of target state simulation val-

ues of the key structural properties of a biological membranes, including mean lipid area and volume, layer thickness, isothermal area compressibility modulus and undulation spectra, that can be attained in hundreds nanoseconds of standard DDM simulation. HREM simulations exhibit a much faster (non physical) lipid diffusion than that driven by the lateral diffusion in conventional runs in standard conditions[58] thus allowing a correspondingly much faster mixing/equilibration rate when simulating heterogeneous systems. This enhanced lipid diffusion provided by our torsional tempering scheme is triggered by a boosted *gauche-trans* conversion in the hot replicas states, easily transmitted, with no apparent bottleneck, to the target thermodynamic state with the correct Boltzmann weight.

HREM on biological membranes allows an unrestrained use of CPU allocation, hence bypassing the restrictions imposed by the Optimal Domain Size in standard DDM parallel approaches whereby scalability can be maintained only at the price of increasing the dimensions of the system. The proposed HREM schemes allow to redistribute the available parallel resources among weak scaling instances, related to the production of concurrent GE trajectories, and strong scaling instances, connected to the force computation in the individual trajectories, in a manner that is mostly convenient for the end-user. On high-end HPC systems, the total simulation time that is attainable using our HREM schemes can easily reach several microseconds per day for moderately sized systems (e.g. for a layer of 64 to 128 lipids per leaflet) operating on at most 2000-3000 cores. We must also mention the fact that GPU accelerators are now becoming to be part of HPC systems and will certainly be an important component in future NUMA multi-cores architectures. In a HREM run on multiple GPU/CPU nodes, for each replica/MPI process, most of the DDM-based strong scaling part (typically the nonbonded forces in the direct lattice) can be efficiently off-loaded to the GPU with a further gain in simulation productivity.[9]

Our torsional tempering approach has been tested using our in-house ORAC code, an hybrid MPI/OpenMP program that has been specifically designed to perform weakly scaling enhanced sampling or non equilibrium techniques on CPU-based HPC platforms. However, the algorithm can be easily implemented on highly efficient and GPU adapted popular molecular dynamics packages as well, such as GROMACS, NAMD[59], AMBER[38] by, e.g., interfacing the executable with powerful plugin extensions,[35] or by modifying the existing topology based HREM scheme.

Finally, we provide on the ORAC site (www.chim.unifi.it/orac), besides

the open source code distributed under the GPL license, a compressed archive containing all the material needed for reproducing the data published in this contributions, including the *Slipids* force field topology and parameters files, starting PDB files for the POPC 17000 atoms system, the input file for HREM simulation with the specification of the 24 replicas torsional tempering scheme and example output HREM files.

## 6. Acknowledgments

The computing resources and the related technical support used for this work have been provided by CRESCO/ENEAGRID High Performance Computing infrastructure and its staff.[7] CRESCO/ENEAGRID High Performance Computing infrastructure is funded by ENEA, the Italian National Agency for New Technologies, Energy and Sustainable Economic Development and by Italian and European research programmes (see www.cresco.enea.it for information).

## 7. Bibliography

[1] Jirasak Wong-ekkabut and Mikko Karttunen. The good, the bad and the user in soft matter simulations. *BBA-Biomembranes*, 1858(10):2529 – 2538, 2016.

[2] J. F. Nagle and S. Tristram-Nagle. Structure of lipid bilayers. *BBA-Rev. Biomembranes*, 1469(3):159–195, 2000.

[3] Max C. Watson, Erik G. Brandt, Paul M. Welch, and Frank L. H. Brown. Determining biomembrane bending rigidities from simulations of modest size. *Phys. Rev. Lett.*, 109:028102, Jul 2012.

[4] Steve Plimpton. Fast parallel algorithms for short-range molecular dynamics. *J. Comput. Phys.*, 117(1):1 – 19, 1995.

[5] See for example "Acceleration and parallelization" Section in the online gromacs[8] documentation at http://www.gromacs.org/ (accessed 22 January 2016).

[6] David E. Shaw. A fast, scalable method for the parallel evaluation of distance-limited pairwise particle interactions. *J. Computat. Chem.*, 26(13):1318–1328, 2005.

[7] G. Ponti, F. Palombi, D. Abate, F. Ambrosino, G. Aprea, T. Bastianelli, F. Beone, R. Bertini, G. Bracco, M. Caporicci, B. Calosso, M. Chinnici, A. Colavincenzo, A. Cucurullo, P. Dangelo, M. De Rosa, P. De Michele, A. Funel, G. Furini, D. Giammattei, S. Giusepponi, R. Guadagni, G. Guarnieri, A. Italiano, S. Magagnino, A. Mariano, G. Mencuccini, C. Mercuri, S. Migliori, P. Ornelli, S. Pecoraro, A. Perozziello, S. Pierattini, S. Podda, F. Poggi, A. Quintiliani, A. Rocchi, C. Scio, F. Simoni, and A. Vita. The role of medium size facilities in the hpc ecosystem: the case of the new cresco4 cluster integrated in the eneagrid infrastructure. In *Proceeding of the International Conference on High Performance Computing & Simulation*, pages 1030–1033. Institute of Electrical and Electronics Engineers ( IEEE ), 2014.

[8] Mark James Abraham, Teemu Murtola, Roland Schulz, Szilard Pall, Jeremy C. Smith, Berk Hess, and Erik Lindahl. Gromacs: High performance molecular simulations through multi-level parallelism from laptops to supercomputers. *SoftwareX*, 1-2:19–25, 2015.

[9] Carsten Kutzner and Szilard Pall and Martin Fechner and Ansgar Esztermann and Bert L. de Groot and Helmut Grubmueller. Best bang for your buck: GPU nodes for GROMACS biomolecular simulations. *J. Comp. Chem.*, 36(26):1990–2008, 2015.

[10] Agnieszka Olyska, Michal Zubek, Martina Roeselova, Jacek Korchowiec, and Lukasz Cwiklik. Mixed dppc/popc monolayers: All-atom molecular dynamics simulations and langmuir monolayer experiments. *BBA-Biomembranes*, 1858(12):3120 – 3130, 2016.

[11] S. J. Marrink, H. J. Risselada, S. Yefimov, D. P. Tieleman, and A. H. de Vries. The martini force field: coarse grained model for biomolecular simulations. *J. Phys. Chem. B*, 111(27):7812–7824, 2007.

[12] H. Fukunishi, O. Watanabe, and S. Takada. On the hamiltonian replica exchange method for efficient sampling of biomolecular systems: application to protein structure prediction. *J. Chem. Phys.*, 116(20):9058–9067, 2002.

[13] Y. Sugita and Y. Okamoto. Replica-exchange molecular dynamics method for protein folding. *Chemical Physics Letters*, 314(1):141–151, 1999.

[14] A. Mitsutake, Y. Sugita, and Y. Okamoto. Generalized-ensemble algorithms for molecular simulations of biopolymers. *Peptide Science*, 60(2):96–123, 2001.

[15] S. Marsili, G. F. Signorini, R. Chelli, M. Marchi, and P. Procacci. Orac: A molecular dynamics simulation program to explore free energy surfaces in biomolecular systems at the atomistic level. *J. Comput. Chem.*, 31(5):1106–1116, 2010.

[16] Wang, Lingle and Friesner, Richard A. and Berne, B. J. Replica Exchange with Solute Scaling: A More Efficient Version of Replica Exchange with Solute Tempering (REST2). *J. Phys. Chem. B*, 115(30):9431–9438, 2011.

[17] Takaharu Mori, Naoyuki Miyashita, Wonpil Im, Michael Feig, and Yuji Sugita. Molecular dynamics simulations of biological membranes and membrane proteins using enhanced conformational sampling algorithms. *BBA-Biomembranes*, 1858(7, Part B):1635 – 1651, 2016.

[18] Xavier Periole and Alan E. Mark. Convergence and sampling efficiency in replica exchange simulations of peptide folding in explicit solvent. *J. Chem. Phys.*, 126(1):014903, 2007.

[19] Weihong Zhang and Jianhan Chen. Efficiency of adaptive temperature-based replica exchange for sampling large-scale protein conformational transitions. *J. Chem. Theory Comput.*, 9(6):2849–2856, 2013.

[20] T. Nagai and Y. Okamoto. Replica-exchange molecular dynamics simulation of a lipid bilayer system with a coarse-grained model. *Mol. Simulat.*, 38(5):437–441, 2012.

[21] Yonglan Liu, Baiping Ren, Yanxian Zhang, Yan Sun, Yung Chang, Guizhao Liang, Lijian Xu, and Jie Zheng. Molecular simulation aspects of amyloid peptides at membrane interface. *BBA-Biomembranes*, 2018.

[22] Tyler J. Harpole and Lucie Delemotte. Conformational landscapes of membrane proteins delineated by enhanced sampling molecular dynamics simulations. *BBA-Biomembranes*, 1860(4):909 – 926, 2018.

[23] T. Mori, J. Jung, and Y. Sugita. Surface-tension replica-exchange molecular dynamics method for enhanced sampling of biological membrane systems. *J. Chem. Theory Comput.*, 9(12):5629–5640, 2013.

[24] Yi Wang, Phineus R. L. Markwick, Csar Augusto F. de Oliveira, and J. Andrew McCammon. Enhanced lipid diffusion and mixing in accelerated molecular dynamics. *J. Chem. Theory Comput.*, 7(10):3199–3207, 2011.

[25] Yinglong Miao, Victoria A. Feher, and J. Andrew McCammon. Gaussian accelerated molecular dynamics: Unconstrained enhanced sampling and free energy calculation. *J. Chem. Theory Comput.*, 11(8):3584–3595, 2015.

[26] G. M. Torrie and J. P. Valleau . Nonphysical Sampling Distributions in Monte Carlo Free-Energy Estimation: Umbrella Sampling . *J. Comp. Phys.*, 23:187–199, 1977.

[27] P. Liu, B. Kim, R. A. Friesner, and B. J. Berne. Replica exchange with solute tempering: A method for sampling biological systems in explicit water. *Proc. Nat. Acad. Sci. USA*, 102(39):13749–13754, 2005.

[28] M. Bizzarri, S. Marsili, and P. Procacci. Intraligand hydrophobic interactions rationalize drug affinities for peptidyl- prolyl cis- trans isomerase protein. *J. Phys. Chem. B*, pages 6193–6201, 2011.

[29] M. Bizzarri, E. Tenori, M.R. Martina, S. Marsili, G. Caminati, S. Menichetti, and P. Procacci. A new perspective on how and why immunophilin fk506-related ligands work. *J. Phys. Chem. Letters*, 2:2834–2839, 2011.

[30] Carlo Guardiani, Giorgio F. Signorini, Roberto Livi, Anna Maria Papini, and Piero Procacci. Conformational Landscape of N-Glycosylated Peptides Detecting Autoantibodies in Multiple Sclerosis, Revealed by Hamiltonian Replica Exchange. *J. Phys. Chem. B*, 116(18):5458–5467, MAY 10 2012.

[31] Maria Raffaella Martina, Eleonora Tenori, Marco Bizzarri, Stefano Menichetti, Gabriella Caminati, and Piero Procacci. The precise chemicalphysical nature of the pharmacore in fk506 binding protein inhibi-

tion: Eltex, a new class of nanomolar fkbp12 ligands. *J. Med. Chem.*, 56:1041–1051, 2013.

[32] Piero Procacci, Marco Bizzarri, and Simone Marsili. Energy-driven undocking (edu-hrem) in solute tempering replica exchange simulations. *J Chem. Theory Comp.*, 10:439–450, 2014.

[33] Oleinikovas, Vladimiras and Saladino, Giorgio and Cossins, Benjamin P. and Gervasio, Francesco L. Understanding Cryptic Pocket Formation in Protein Targets by Enhanced Sampling Simulations. *J. Am. Chem. Soc.*, 138(43):14257–14263, 2016.

[34] Giovanni Bussi. Hamiltonian replica exchange in GROMACS: a flexible implementation. *Mol. Phys.*, 112(3-4):379–384, 2014.

[35] Gareth A. Tribello, Massimiliano Bonomi, Davide Branduardi, Carlo Camilloni, and Giovanni Bussi. Plumed 2: New feathers for an old bird. *Comput. Phys. Comm.*, 185(2):604 – 613, 2014.

[36] J. B. Klauda. Laboratory of molecular & thermodynamic modeling. http://terpconnect.umd.edu/ jbklauda/research/download.html, 2018.

[37] 2018. In the present force field variant, the standard AMBER fudge factors were applied to *all* 14 interactions and only X-H bonds were constrained.

[38] Romelia Salomon-Ferrer, David A. Case, and Ross C. Walker. An overview of the amber biomolecular simulation package. *Wiley Interdisciplinary Reviews: Computational Molecular Science*, 3(2):198–210, 2013.

[39] J. P. M. Jämbeck and A. P. Lyubartsev. Derivation and systematic validation of a refined all-atom force field for phosphatidylcholine lipids. *J. Phys. Chem. B*, 116(10):3164–3179, 2012.

[40] M. Parrinello and A. Rahman. Polymorphic transitions in single crystals: A new molecular dynamics method. *J. Appl. Phys.*, 52(12):7182–7190, 1981.

[41] S. Nosé. A unified formulation of the constant temperature molecular dynamics methods. *J. Chem. Phys.*, 81(1):511–519, 1984.

[42] W. G. Hoover. Canonical dynamics: equilibrium phase-space distributions. *Phys. Rev. A*, 31(3):1695, 1985.

[43] U. Essmann, L. Perera, M. L. Berkowitz, T. Darden, H. Lee, and L. G. Pedersen. A smooth particle mesh ewald method. *J. Chem. Phys.*, 103(19):8577–8593, 1995.

[44] W. L. Jorgensen, J. Chandrasekhar, J. D. Madura, R. W. Impey, and M. L. Klein. Comparison of simple potential functions for simulating liquid water. *J. Chem. Phys.*, 79(2):926–935, 1983.

[45] Daniel J. Sindhikara, Daniel J. Emerson, and Adrian E. Roitberg. Exchange often and properly in replica exchange molecular dynamics. *J. Chem. Theory Comput.*, 6(9):2804–2808, 2010.

[46] Berk Hess, Carsten Kutzner, David van der Spoel, and Erik Lindahl. Gromacs 4: algorithms for highly efficient, load-balanced, and scalable molecular simulation. *J. Chem. Theory Comput.*, 4(3):435–447, 2008.

[47] R. Hayashi and S. Horiguchi. Efficiency of dynamic load balancing based on permanent cells for parallel molecular dynamics simulation. In *Proceedings 14th International Parallel and Distributed Processing Symposium. IPDPS 2000*, pages 85–92, 2000.

[48] Consorzio Interuniversitario del Nord est Italiano Per il Calcolo Automatico (Interuniversity Consortium High Performance Systems) http://www.cineca.it (accessed 22 January 2018).

[49] Piero Procacci. Hybrid mpi/openmp implementation of the orac molecular dynamics program for generalized ensemble and fast switching alchemical simulations. *J. Chem. Inf. Model.*, 56(6):1117–1121, 2016.

[50] P. Procacci, T. A. Darden, E. Paci, and M. Marchi. Orac: A molecular dynamics program to simulate complex molecular systems with realistic electrostatic interactions. *J. Computat. Chem.*, 18(15):1848–1862, 1997.

[51] Piero Procacci, Tom Darden, and Massimo Marchi. A very fast molecular dynamics method to simulate biomolecular systems with realistic electrostatic interactions. *J. Phys. Chem.*, 100(24):10464–10468, 1996.

[52] M. R. Shirts and J. D. Chodera. Statistically optimal analysis of samples from multiple equilibrium states. *J. Chem. Phys.*, 129:124105, 2008.

[53] P. Procacci. Multiple bennett acceptance ratio made easy for replica exchange simulations. *J. Chem. Phys.*, 139:124105, 2013.

[54] N. Kučerka, M.-P. Nieh, and J. Katsaras. Fluid phase lipid areas and bilayer thicknesses of commonly used phosphatidylcholines as a function of temperature. *BBA-Biomembranes*, 1808(11):2761–2771, 2011.

[55] N. Kučerka, S. Tristram-Nagle, and J. F. Nagle. Structure of fully hydrated fluid phase lipid bilayers with monounsaturated chains. *J. Membrane Biol.*, 208(3):193–202, 2006.

[56] H. Binder and K. Gawrisch. Effect of unsaturated lipid chains on dimensions, molecular order and hydration of membranes. *J. Phys. Chem. B*, 105(49):12378–12390, 2001.

[57] Erik G. Brandt, Anthony R. Braun, Jonathan N. Sachs, and Olle Edholm John F. Nagle. Interpretation of fluctuation spectra in lipid bilayer simulations. *Biophys J.*, 100:2104–2111, 2011.

[58] Radek Mach and Martin Hof. Lipid diffusion in planar membranes investigated by fluorescence correlation spectroscopy. *BBA-Biomembranes*, 1798(7):1377 – 1391, 2010. Microscopy Imaging of Membrane Domains.

[59] J. C. Phillips, R. Braun, W. Wang, J. Gumbart, E. Tajkhorshid, E. Villa, C. Chipot, L. Skeel, and K. Schulten. Scalable molecular dynamics with namd. *J. Comput. Chem.*, 26:1781–1802, 2005.